Surface-based Methane Monitoring and Measurement Network Pilot Demonstration: Findings from Project Astra Phase I

January 31, 2023

SUBMITTED BY

The University of Texas at Austin
Center for Energy and Environmental
Resources M/C R7100 at EME
10500 Exploration. Way
Austin, Texas 78758

PRINCIPAL INVESTIGATOR

David Allen
allen@che.utexas.edu

SUBMITTED TO

U.S. Department of Energy
National Energy Technology Laboratory

Contents

Summary

Project Astra is testing the effectiveness of a shared network of fixed methane emission monitors in the Permian Basin oil and gas production region in West Texas. The Project Astra partnership, formed in 2020, is led by the University of Texas Center for Energy and Environmental Resources, and includes Chevron, the Environmental Defense Fund, ExxonMobil, GTI Energy, Microsoft, Pioneer Natural Resources, and SLB. Since 2020, the goal of the Project has been to test the effectiveness of a shared network of fixed methane emission monitors in detecting methane emissions from oil and gas operations. Through 2023, the project proceeded through three stages. An initial stage evaluated the performance of methane sensing systems in nine months of field testing. In a second stage, based on the performance characteristics of the sensing systems demonstrated in field testing, network designs were developed and a network design with multiple redundancies was created. In a third stage, the network was deployed and operated, beginning in February 2022.

This report documents the development of Project Astra from 2020 through 2023. Sections of the document, summarized below, describe site selection, sensor testing, network design, data analytics, and overall performance of the network. Beginning in late 2023, Project Astra entered a second Phase, which will be documented in subsequent reports.

Site selection The Project Astra field deployment encompasses approximately 50 sites in a ~10 km^2 area; the Permian Basin site was selected based on its strong, steady winds, and its well density and productivity. The selected area, near Midland Texas, contains production sites that are representative of the Basin.

Sensor testing Multiple commercially available sensing systems were field tested; two types of high precision infrared sensing systems and one moderate precision metal oxide semiconductor sensing system were chosen for network deployment

Network design The network was designed to simultaneously test (i) a dense network of moderate resolution sensors and (ii) a sparse network of high resolution sensors, with both networks designed to cover the entire test region. Some individual sites were equipped with multiple sensors to enable comparison of single and multiple site deployments. Network design software based on dispersion modeling was developed and tested.

Data analytics Software systems were developed and tested for background correction and emission event detection. On-going work is developing tools for source attribution, quantifying emission event durations, and reducing uncertainty in emission rate quantification.

Overall performance The sub-systems that most constrain the overall performance of the network performance are the data analytics capabilities. On-going work is expanding those capabilities.

1. Introduction

Project Astra is testing the effectiveness of a shared network of fixed methane emission monitors in the Permian Basin oil and gas production region in West Texas. The Permian basin was chosen for this demonstration because it is the largest oil and gas production region (by volume of production) in the United States, because the region has simple topography and strong and persistent winds and because the proximity oil and gas production sites in the Permian Basin enhances the advantages of a shared network of sensors. Because of the proximity of sites, emissions can be detected without having multiple sensors surrounding every site. Compared to isolated sites requiring fixed sensors located at multiple cardinal directions (e.g., sensors north, south, east and west of each site), sensors in the Permian Basin can be located at nearby sites (e.g., sites to the north, south, east and west of a central site) to replace some of the information that would be provided by multiple sensors for isolated sites.

The Project Astra partnership, formed in 2020, is led by the University of Texas Center for Energy and Environmental Resources, and includes Chevron, the Environmental Defense Fund, ExxonMobil, GTI Energy, Microsoft, Pioneer Natural Resources, and SLB. The initial goal of the Project was to test the effectiveness of a shared network of fixed methane emission monitors in detecting methane emissions from oil and gas operations. Through 2023, the project proceeded through three stages. An initial stage evaluated the performance of methane sensing systems in nine months of field testing. Based on the performance characteristics of the sensing systems demonstrated in field testing, network designs were developed and a network design with multiple redundancies was created. The network deployment began in February 2022. Data ingestion systems and emission detection algorithms were developed, and the network was successfully operated throughout 2023.

In October 2023, the U.S. Department of Energy funded a next phase of Project Astra. The objectives of Phase 2 of Project Astra are to:

- *Extend the Project Astra network to a demonstration of a scalable "basin-wide" platform* The types of facilities sampled will be expanded from a contiguous group of approximately 50 sites that are primarily oil and gas production pads, to include gas gathering and boosting sites and gas processing sites. The gas processing and gathering and boosting sites will be individual sites that are not contiguous with each other or the existing network.
- *Advance the detection and quantification capabilities of sensing technologies* Project Astra's initial sensing network includes multiple types of fixed position ground sensing systems to detect, but not necessarily quantify emissions. Phase II of the project will continue work on emission detection, focusing on characterizing the frequency and duration of emission events, and will assess the ability of the network to quantify emissions.
- *Support emission inventory improvements* Expanding detection and quantification capabilities will enable the development of emission factors, region specific emission inventories, and characterization of the magnitudes, frequencies and durations of emission events.
- *Demonstrate advanced data analytics and accelerate and automate responses to network emission detections* Project Astra currently manually performs data analytics on sensor signals, identifying network detections on a roughly weekly basis. Detections are discussed

with operators and analyses are performed based on operator provided process data, site log information and on-site follow-up. These data analytics will be automated and compared with process data and site activity data.

- *Inform the development of Integrated Methane Modeling Platform Designs* By documenting its processes and analysis tools, Project Astra will help inform future monitoring system designs.
- *Develop education and training programs for workforce development* Operation of methane emission monitoring systems will require training. Training programs developed through this program will contribute to workforce development.

The remainder of this document summarizes the status of Project Astra and documents its development from 2020 through 2023. Sections of the document describe site selection, sensor testing, network design, data analytics, and overall performance of the network.

2. Site selection and regional meteorology

2.1 Site characterization

The initial Project Astra test network is located in west Texas in the Permian Basin oil and gas production region. Site selection criteria, for locations within the Permian Basin included:

- Representative oil and gas production volumes
- Representative well densities
- Representative methane emissions by magnitude and source type
- Access to regional air travel
- Availability of sites for all three operators (Chevron, ExxonMobil, and Pioneer) participating in Project Astra in a contiguous region

Based on these criteria, a site near the city of Midland was selected for the Project Astra demonstration.

The initial demonstration region contains a total of 74 active wells on approximately 50 pads, collectively producing 9302 Mscf/day of gas and 2254 barrels per day of oil, as of May 2023. The average production rate per well is 125.7 Mscf/d of gas and 30.5 barrels per day of oil. These production rates are broadly representative of production rates in the Permian Basin (156 Mscf/day of gas and 38.3 barrels/day of oil per well). Average production rates in Midland County are slightly higher, on average, than in the entire Permian Basin, at 291 Mscf/d of gas production and 83.5 barrels/day of oil production per well. The distributions of production rates for gas and oil, for the wells in the demonstration region, wells in Midland County, and wells in the Permian Basin, that were actively producing in May 2023, is shown in Figure 2-1.

Figure 2-1. Distribution of oil and gas production rates per well in the demonstration region, Midland County, and the Permian Basin in May 2023.

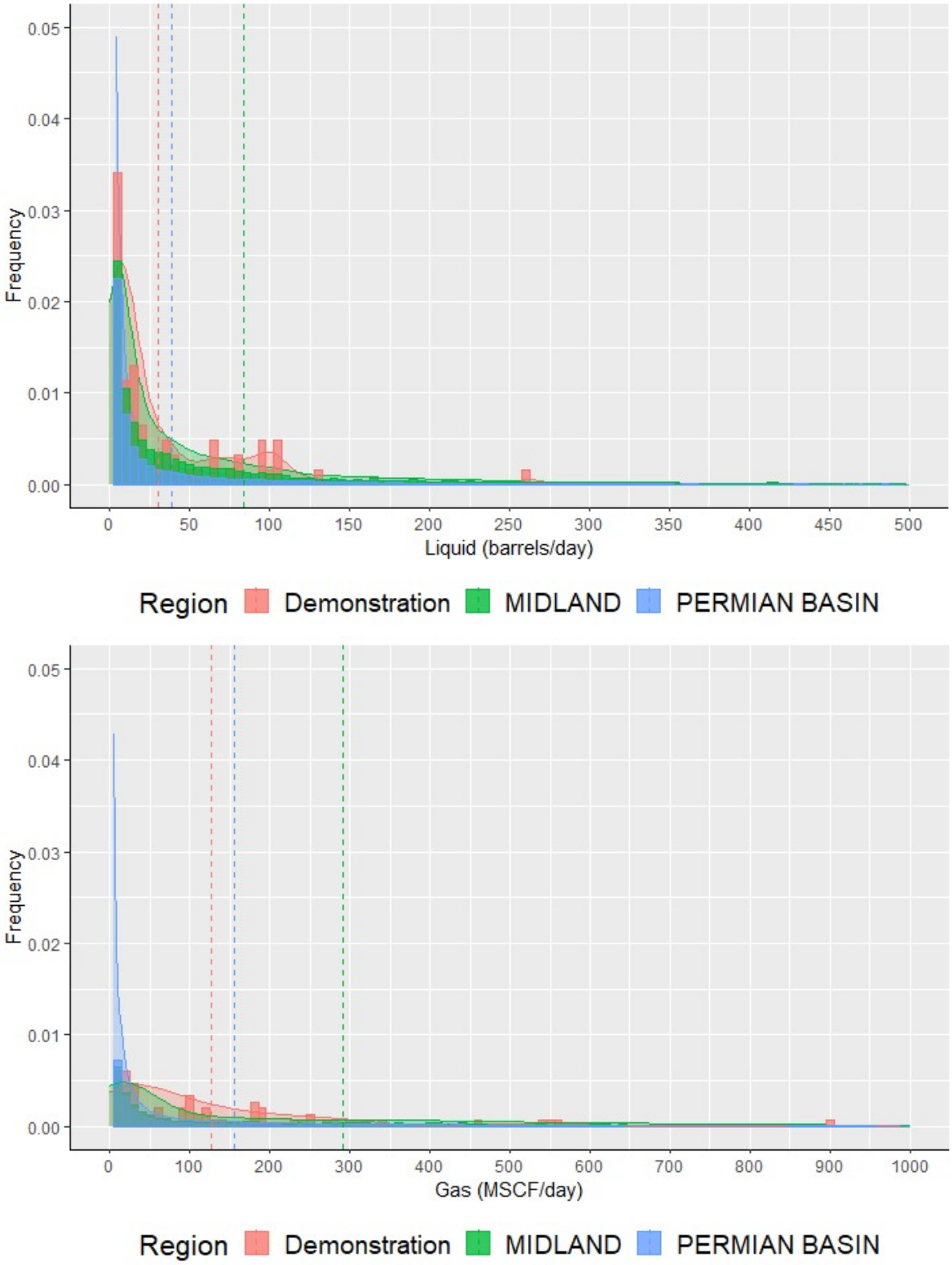

The area covered by the contiguous demonstration region is 7.32 km^2. This area is defined by a convex polygon including all the pads in the network. With 74 actively producing wells (in May 2023), the well density is 10.1 wells/km^2, which is higher than the Midland well density of 3.3 wells/km^2 and considerably higher than the Permian Basin well density of 0.55 wells/km^2.

The well sites in the region include single well pads with limited liquids handling equipment, single well pads with associated liquids handling equipment and flares, and tank battery sites with liquids and gas handling equipment for multiple wells located on other pads.

2.2 Regional meteorology and topography

The Permian basin is characterized by persistent winds with average wind speeds of approximately 8-9 miles per hour. Figure 2-2 shows the seasonal distributions in wind directions, as recorded by a Continuous Air Monitoring Station (CAMS) maintained and operated by the Texas Commission on Environmental Quality (TCEQ, 2024). Wind directions in the spring and summer are primarily from the southeast to southwest. In the fall and winter, wind directions are more variable; in all seasons, wind speeds average 8-9 miles per hour. Calm periods are infrequent with less than 5% of observational hours having wind speeds below 3 miles per hour in 2019 (Figure 2-3).

These distributions of wind speeds and directions indicate that sensing systems placed on the southern boundary of pads will generally sample upwind conditions, while sampling systems on the northern boundaries of pads will generally detect emissions from the pads.

Figure 2-2. Wind roses documenting wind speed and direction frequency distributions, binned by quarter, using hourly TCEQ CAMS observational data for year 2019 (TCEQ, 2024)

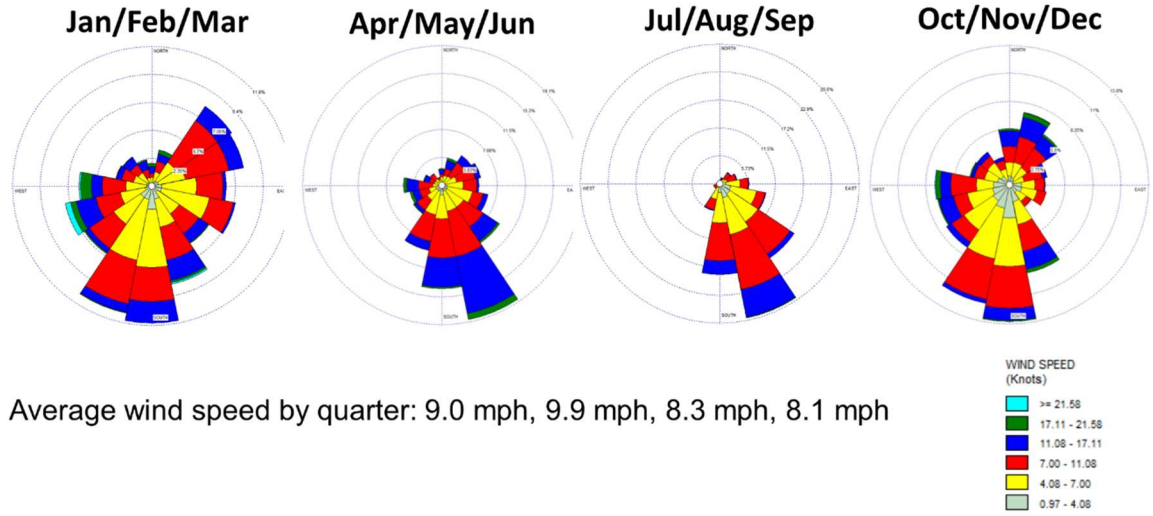

Figure 2-3. Annual frequency distribution of hourly CAMS 47 wind speeds during 2019.

Number of valid hours during 2019: 8749 hours

Median: 8.2 mph
Average: 8.8 mph
Maximum: 34 mph

~90% of hourly observations range 3 to 17 mph

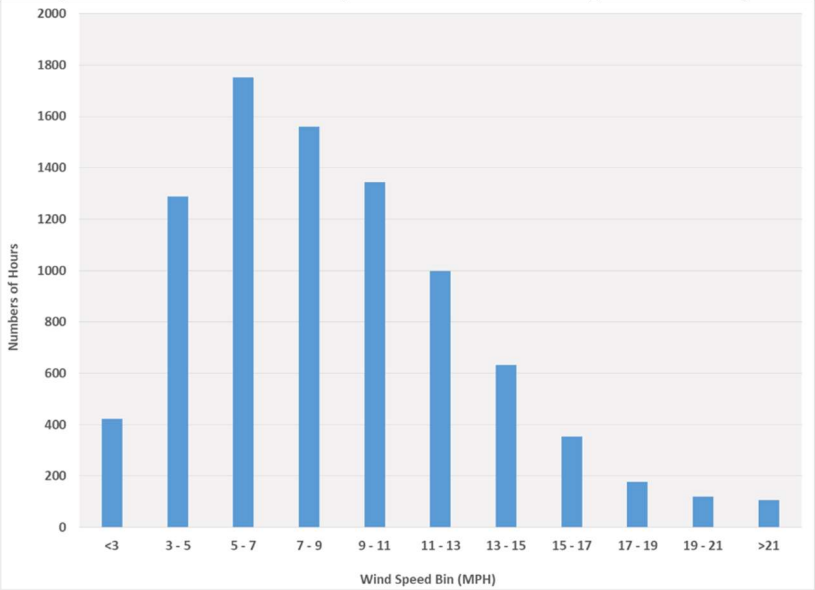

3. Sensor testing and intercomparison

3.1 Findings from sensor field testing

Seven methane sensing technologies were deployed in West Texas' Permian Basin. Sensors were operated unsheltered from October 29, 2020 through June 22, 2021. The field test site is shown in Figure 3.1.

Figure 3-1. Field intercomparison site used in Project Astra to evaluate four methane sensing systems.

Sensor accuracy and precision were evaluated by conducting unannounced single blind challenges with certified gases and by comparison with continuous measurements made by an Aerodyne Research Incorporated (ARI) QC-TILDAS instrument (Quantum Cascade-Tunable Infrared Laser Differential Absorption Spectrometer), operated by The University of Texas (UT) and located within the trailer shown in Figure 3-1. Data accuracy was judged based on the measured sensor concentration compared with known challenge gas concentrations and compared with coincident, collocated air measurements by the ARI QC-TILDAS.

The metrics used in evaluating the certified gas challenges were as follows:

- Rise Speed – estimated time duration in seconds for the measured concentration to reach 2/3 of the way to the maximum concentration recorded during the challenge.
- Decline Speed – estimated time duration in seconds for the measured concentration to reach 2/3 of the way to the estimated background concentration.
- Percent Target Concentration Met – the maximum concentration reached compared to the coincident QC-TILDAS mean concentration during the challenge.
- Integration Relative to QC-TILDAS – The concentrations are integrated over time series for the TILDAS and the sensor during the challenge.

Details of the intercomparison are provided in by Torres, et al. (2022). A brief summary is provided here.

Three of the seven sensing systems tested had performance that did not merit detailed analyses. Of the remaining four sensors (Aeris, Canary, Quanta3 and Scientific Aviation), the Aeris and Quanta3 samplers had time responses in the challenge gas tests comparable to the QC-TILDAS instrument,. The Canary and Scientific Aviation devices responded more slowly, but still with a 1-2 minute response time. The integrated areas for the Aeris, Quanta3 and Scientific Aviation instruments were all typically within ±20% of the integrated TILDAS response. The Canary sensor had time integrated responses that were typically 50-70% of the TILDAS response. Data capture completeness, defined as the fraction of time for which valid measurements were made over the test period, was >80% for the four sensors. The Scientific Aviation sensor had 100% data completeness over the nine months of testing.

The measurements of the sensors were also compared to the measurements of the QC-TILDAS in the time periods between certified gas challenges. For the Aeris, Quanta3 and Canary sensors, slopes of the best linear fit of the sensor concentration to the QC-TILDAS concentration, which had its sample inlet 1-2 meters from each of the sensors being tested, were generally >0.6, for concentrations averaged over one minute. Linear correlation coefficients (R^2) of these two concentration measurements were generally >0.6. The Scientific Aviation sensor showed baseline bias, however, when the metric used for comparison with the QC-TILDAS was the difference between instantaneous concentration and daily minimum concentration, the bias in the Scientific Aviation sensor largely disappeared during the nine months of field testing.

Based on the results of the sensor intercomparison and the availability of multiple sensing systems for field deployment in the pilot, the Aeris, Quanta3 and Scientific Aviation sensing systems were chosen for use in the Project Astra pilot project. Table 3-1 and Figures 3-2 to 3-4 summarize the features of these three sensing systems.

Table 3-1. Sensing systems selected for pilot deployment

	Quanta 3	Aeris	Scientific Aviation
Measurements	Configured to measure methane only. Sensor unit also records barometric pressure, temperature, and humidity	MIRA technology measures ethane and methane at <1ppb/s sensitivity level, plus H_2O vapor and dry mole fractions. C2:C1 ratio can be used to discriminate sources.	Multi-gas, any reducing gas; calibrated for methane
Footprint/Space	30 x 30 inches	6-9 ft^2	1'x1'
Temporal resolution	1 sec.	0.5 - 1.0 sec.	0.2 sec.
Detector	Near infrared laser absorption spectroscopy sensor based on tunable diode laser spectroscopy	Direct absorption mid-IR spectroscopy in the 3 micron region.	Metal oxide sensor
Sensitivity/Range	Ambient (2 ppm) to 500 ppm (optimized for high sensitivity)	1ppb level to % concentration levels.	500 ppb over background to 5000 ppm
Accuracy	Field precision is better than 20 ppb; Accuracy is rated at ~20% at background concentrations (2 ppmv)	methane and ethane: 600ppt/s sensitivity in both Pico and Ultra version of MIRA gas analyzers. Accuracy: 1-2ppb drift long-term in Ultra analyzers for methane, 10-30ppb drift in Pico series. Ethane: <1ppb drift in Ultra Series and 7ppb drift max typical in Pico series.	CH_4 precision: ± 60 ppb for a 1-minute average CH_4 accuracy: ±(1 ppm + 15%)

The Aeris Technologies sensing system uses a mid-infrared laser-based gas analyzer and has a sample flow rate of approximately 0.3-0.5 lpm. The analyzer was configured for 1 Hz data sampling. Additional information is available at www.aerissensors.com. Figure shows the installed Aeris sensor

Figure 3-2. Aeris sensing system

The Quanta3 sensing system measures methane using tunable laser diode spectroscopy technology. The system makes one measurement per second and reports data at the same frequency via 4G/LT cellular modem to a proprietary cloud platform. The system is powered by a solar battery recharged by solar panels. For additional information is available at https://www.quanta3.com. Figure shows the installed Quanta 3 sensing system.

Figure 3-3. Quanta 3 sensing system

Figure 3-4. Scientific Aviation sensing system (SOOFIE)

The Scientific Aviation unit is a multi-gas sensor using metal oxide semiconductor technology. The system makes 5 voltage measurements per second and averages the 300 voltage measurements from each minute to report one voltage measurement per minute via LTE cellular modem to a cloud server. Voltage readings are converted to concentration measurements on the server. The system is powered by a battery recharged by an integrated solar panel. A photo of the installed Scientific Aviation SOOFIE sensor appears in Figure 3-4.**Error! Reference source not found.** Additional information is available at https://www.scientificaviation.com/soofie/

3.2 Sensor intercomparisons during Project Astra pilot deployment

To continue sensor intercomparisons the three sensing systems selected for the Project Astra pilot demonstration were deployed with multiple co-locations of sensing systems. Additional intercomparisons of sensing systems are underway. Table 3-2 summarizes data completeness data for 2023 (fraction of time sensing system produced data that passed initial quality assurance screening). The percentages reported in Table 3-2 are data completeness metrics averaged over all sensing systems of a given type (Aeris, Quanta3 and Soofie).

Table 3-2. Data completeness for 2023 for the three sensing systems

	Monthly data completeness (%) by sensor type for 2023, Averaged over all sensing systems of each type in the network		
	Aeris	**Quanta3**	**Soofie**
January 2023	46.1	83.1	87.8
February 2023	19.6	83.1	89.0
March 2023	34.6	97.0	89.5
April 2023	35.7	99.3	89.7
May 2023	24.9	94.4	91.9
June 2023	9.5	98.4	95.0
July 2023	21.2	99.3	96.4
August 2023	17.0	99.7	94.8
September 2023	9.7	98.6	94.0
October 2023	6.9	97.9	96.8
November 2023	32.6	99.1	96.7
December 2023	60.4	87.9	96.7

4. Network Design

Network design proceeded through a series of steps. An initial step determined the sensing system density, expressed as sensors per site, required to be able to detect emissions throughout the network. After determining the approximate sensing system density, sensing system locations were selected, accounting for physical constraints on system deployment such as avoiding locating sensing systems in the direct vicinity of site equipment. Finally, additional analyses were performed to assess the sensitivity of emission detection to the exact placement of sensing systems on the sites and dispersion characteristics of the emissions, such as plume buoyancy and emission release height.

4.1 Sensor density

To evaluate the number of sensors required per site in the Project Astra pilot network, atmospheric dispersion of methane emissions was modeled for a simulated network containing 26 oil and gas production sites. Virtual methane sensors were placed at 24 of the 26 sites, with at most one sensor per site. Emissions were simulated from each of the 26 oil and gas production sites, over four week-long meteorological episodes, representative of winter, spring, summer and fall meteorology in the Permian Basin.

In order to determine the density of sensing systems required in a network, a detection objective, which includes a threshold emission rate and a time to detection must be specified. For the initial sensor density calculation, the goal was to determine the sensing system density that would be required to detect an emission rate of 10 kg/hr within one week of the onset of emissions. These values for threshold and time to detection were selected to be consistent with the types of specifications anticipated by the Project Astra team for regulatory applications. When regulations were finalized by the EPA in December 2023 (US EPA, 2023), the Project Astra team began the process of re-examining these thresholds.

Once a detection goal is established, the limit of detection of the sensing system must be defined. For this initial sensor density calculation, it was assumed that a sensing system could detect a concentration enhancement of 1 ppm that persisted for one minute. Additional definitions of event detection have been investigated and are described in Section 5. In the design calculations, the detection threshold scales directly with emission rate. For example, a network capable of detecting emissions of 10 kg/hr within a week of onset of emissions, using sensing systems able to detect 1 ppm concentration enhancements ,is equivalent to a network capable of detecting emissions of 100 kg/hr within a week of onset of emissions, using sensing systems able to detect 10 ppm concentration enhancements.

The detailed analyses are described by Chen, et al. (2022). In summary, less than 1 sensor per site was required to detect emissions from all sites in the network within a week, if emissions were continuous at a rate of 10 kg/hr. If emissions were intermittent (1 minute of emissions per hour), less than one sensor per site was still capable of detecting emissions at all 26 sites in all four seasonal episodes (spring, summer, fall and winter) if the detection threshold was lowered to 500 ppb. These results are specific to the site density of the region modeled in the simulations, so a region with less dense sources was also modeled. Comparable ratios of sensors to sites were sufficient to detect emissions from a less dense group of sources, however, more sensors are required to detect lower emission rates. Overall, this site density analysis demonstrated that for

the conditions in the test region in the Permian Basin, less than one continuous monitor per site is likely to be capable of consistently detecting emissions in the range of 5-10 kg/hr within a week if a methane enhancement of 1 ppm for one minute can be reliably detected. Equivalently, one continuous monitor per site is likely to be capable of consistently detecting emissions in the range of 50-100 kg/hr if a methane enhancement of 10 ppm for one minute can be reliably detected.

4.2 Initial network configuration

A requirement of one sensing system per site leads to a conceptual configuration of sensing system placement shown in Figures 4-1 and 4-2. Figure 4-1 shows a conceptual mapping of the entire network. Pad sites are indicated by a black circle and may be small with only a wellhead and only a few other pieces of equipment, or may be large and contain multiple tanks, separators, compressors and other potential sources. Based on the need for one sensor or less per site, sensing systems were deployed to yield three configurations. Two of the networks, operating in parallel, are designed to monitor emissions from the entire domain, encompassing approximately 50 sites distributed relatively uniformly throughout a ~10 km^2 area. One of these networks consists of 42 moderate resolution sensors (~100-500 ppb precision) and a second network consists of 12 high resolution sensors (~10 ppb precision). These are shown conceptually as high resolution and moderate resolution sensing systems in Figure 4-1. Both systems are designed to simultaneously monitor the same region, allowing inter-comparisons between moderate resolution-high spatial density networks and high resolution-low spatial density networks. Moderate resolution sensors are co-located with all high-resolution sensors, also allowing for continued direct intercomparisons between sensor types.

A final monitoring network, also operating in parallel, is designed to examine emissions at individual sites (rather than the network of ~50 sites), with at least three sensing systems locations at each of the individual sites being monitored. This is shown conceptually in Figure 4-2.

With three parallel networks deployed in the same region, there is redundancy in sampling locations and capabilities in the current network, and the network allows for inter-comparison of multiple monitoring strategies and multiple sensing system types. The number of sensors deployed in each network was greater than minimum number required based on the modeling analyses, so that multiple strategies for deploying sensors could be evaluated. Sensor locations were constrained to be on operator owned pads, since lease agreements often would not allow placement of sensors off the pad. The sensor networks have been in operation since March, 2022.

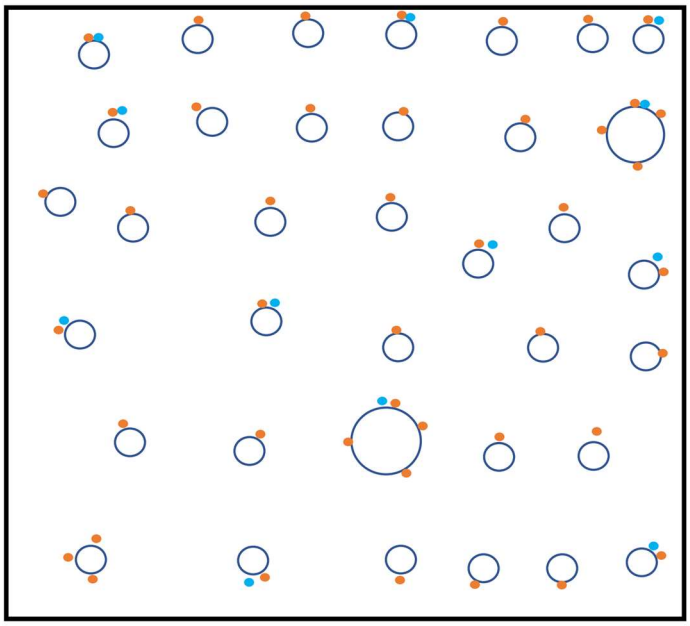

Figure 4-1. Conceptual mapping of the Astra network. Pad sites are indicated by a black circle and may contain multiple sources. Moderate resolution sensors are indicated in orange and high resolution sensors are indicated in blue.

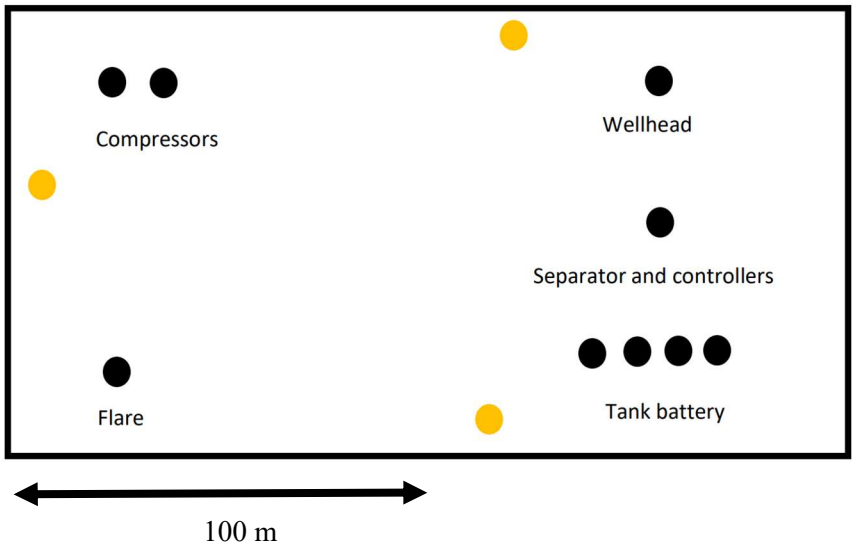

Figure 4-2. Conceptual mapping of a single site with multiple sensors. Sources are indicated by black dots and sensors are indicated by orange dots. Note that sensor locations are frequently constrained by equipment positioning on pads.

4.3 Sensitivity of network design to time to detection and source characteristics

The sensing systems deployed in Project Astra operate continuously, however, a discrete number of sensors, such as those shown in Figures 4-1 and 4-2, will not be able to detect emissions from all sources at all times. Emission plumes may pass between sensors or above sensors. A network's efficiency in detecting emissions will depend on meteorological conditions, sensor detection limits, the number of sensors deployed, and sensor placement strategies. The Project Astra team developed an approach to assess the effectiveness of sensor networks in detecting emission events. The method is described in detail by Chen, et al. (2023a,b), and is demonstrated here using a case study of a group of 9 different sources at varying heights and locations on a single pad. Using site specific meteorological data and dispersion modeling, the time periods when a sensing system is unable to detect emission events was determined.

Figure 4-3 shows the prototypical site configuration used in the analysis. This configuration is typical of a tank battery, which includes compression and liquid handling and processing equipment for multiple production wells. The sources include tanks, compressors, a flare, dehydrators, pumps, separators (including associated pneumatic devices), and other equipment. A detailed description of the sources on this prototypical site are provided by Chen, et al. (2023a). Of the 9 sources, some are non-buoyant and release emissions near ground level. Other sources (tanks) have non-buoyant emissions that are released at ~5 m above ground level (AGL). Still other sources (compressor exhaust and flares) release emissions at higher elevations and the releases are buoyant. Also shown in Figure 4-3 are four potential sensor locations. The placements were restricted to the periphery of the site. This is often a practical constraint encountered in the field, so that the sensing systems do not interfere with operator access to equipment. The sensor locations selected were the placements that led to the highest averaged probability of detection across the 9 sources at the site. These sensor locations might not be ideal for individual emission source locations at different positions around the pad; however, this is a trade-off that is typical of field deployments.

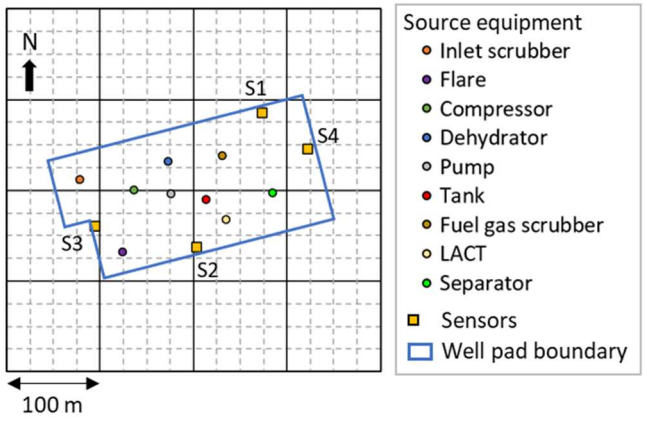

Figure 4-3. A typical tank battery site configuration with multiple emission source locations and four sensor locations arrayed around the perimeter of the pad.

Dispersion modeling was performed using the same methodologies reported by Chen, et al. (2023a). Briefly, CALPUFF v7.2.17 was used to estimate concentrations at sensor sites with a 1 min time resolution. The primary meteorological data set was 1-minute wind speed and direction

data collected by six meteorological stations in the Project Astra network. Meteorological data from March 26th to April 8th 2022 (local standard time, LST) was selected as the primary data set for this work, as the wind directions across this 2-week period are broadly representative of annual weather patterns (Chen, et al., 2023a). Dispersion of sources emitting methane at a rate of 100 kg/hr were modeled.

If the dispersion modeling results indicated that a sensor would be exposed to a background-corrected methane enhancement of 10 ppm or more for at least 1 min, the emission was assumed to be detected. The detection threshold of 10 ppm was based on the performance of multiple types of sensors deployed in field testing in the Permian Basin. The primary event detection threshold of a methane enhancement of 10 ppm over a one minute period could also be supplemented with a persistence criterion. Chen, et al. (2023b) present an analysis that combines a detection criterion of a 10 ppm methane enhancement for one minute with an average 5 ppm enhancement over a 15 minute period.

Table 4-1 shows the average time to detection for each source in Figure 4-3, if one (S1 in Figure 4-3), two (S1, S2 in Figure 4-3), three (S1, S2, S3 in Figure 4-3) or four sensors are deployed. Table 1 reports average times until detection for 100 kg/hr release events starting at a random time. Sources with emissions that are buoyant (e.g., compressor exhaust and flares) have longer times to detection than non-buoyant emissions. The average time to detection averaged over all sources is 12 hours. The full range of times until detection range from 0 minutes, if the sensor is able to detect the emission at the moment it starts, to a maximum of ~83 hours (3.5 days), for the compressor if only one sensor is on the site. More details are provided by Chen, et al., 2023b.

Table 4-1. Average time to detection for a large emission event at a tank battery site

Source	Time (hours) until detection for different numbers of sensors on the model site			
	1 Sensor	**2 Sensors**	**3 Sensors**	**4 Sensors**
Compressor	25	16	13	13
Dehydrator	7.9	4.3	3.0	2.7
Flare	19	16	11	7.4
Fuel gas scrubber	5.6	3.2	2.4	1.6
Inlet scrubber	12	7.3	5.8	5.8
LACT	9.6	3.1	2.9	2.2
Separator	9.7	3.2	3.1	2.0
Tank	9.2	3.6	2.8	1.9
Pump	7.2	4.0	2.7	2.2
Average over all sources	12	6.8	5.2	4.3
Minimum	5.6	3.1	2.4	1.6
Maximum	25	16	13	13

The average values of time to detection of a large release event for this prototypical complex site provide guidance on how effective continuous monitoring systems could be in constraining the time to detection of large release events. The overall duration of an event is the sum of the time to detection and the time to mitigation. Since the time to mitigation will be determined by the relatively well-defined time between detection and the mitigation action, time to detection represents the largest uncertainty in estimating the duration of a large event. The analysis shows that even deployment of just one sensor per site would lead to an average time to detection, from multiple sources, of roughly a day or less.

5. Data analytics

The data streams from the sensors deployed in the test region have been integrated into a data network. In the case of the Scientific Aviation metal oxide semiconductor sensor, a background correction was applied to the signal; the Quanta3 and Aeris sensing systems did not require background corrections. Once processed and background corrected, the sensing system signals were searched for event detections. Meteorological data and dispersion modeling were used to identify potential sources, and to perform preliminary characterization of the duration of select events.

5.1 Sensor background corrections and event detection

Data from the field intercomparison was used to determine whether the sensing systems would require background correction. The background in the field intercomparison was determined using continuous (1 Hz) measurements made by an Aerodyne Research Incorporated (ARI) QC-TILDAS instrument (Quantum Cascade-Tunable Infrared Laser Differential Absorption Spectrometer), operated by The University of Texas (UT) and located within the trailer shown in Figure 3-1. The Aerodyne QC-TILDAS instrument was deployed in a multi-port sampling mode. The multiple ports sampled ambient methane concentrations at nine locations on the sampling site, within approximately two meters of the inlet to each sensor. Each sample port had a dedicated sampling line and ambient air was continuously drawn through the lines by a vacuum pump. All of the individual sampling lines were delivered, with continuous sample flow, to a multi-port sampling valve and then, sequentially, to the QC-TILDAS instrument. The timing of the sequencing was designed to rapidly cycle through the sample locations. Every 12 minutes, the QC-TILDAS switched its sample line channel from one sensor to another. A 12-minute period was selected to balance the small amount of data loss as sample lines are switched with the different measurement durations among the sensors, with the practical need to simplify later matching up QC-TILDAS measurements with the sensor measurements. Details are described by Torres, et al. (2022).

Figure 5-1 shows representative data, comparing the signals from the QC-TILDAS to the signals from the Aeris, Quanta3 and Scientific Aviation sensors. Data from a representative week of sampling is shown. Because of the sequential sampling, the comparisons between individual sensors and the QC-TILDAS are for different time periods during the week-long period,

The data shown in Figure 5-1, and other data collected throughout the sampling (Torres, et al., 2022) indicated that the Aeris and Quanta3 systems (infrared detection) would not require a background correction. The Scientific Aviation system, however, with its metal oxide semiconductor sensor, showed a baseline bias that was related to atmospheric water content.

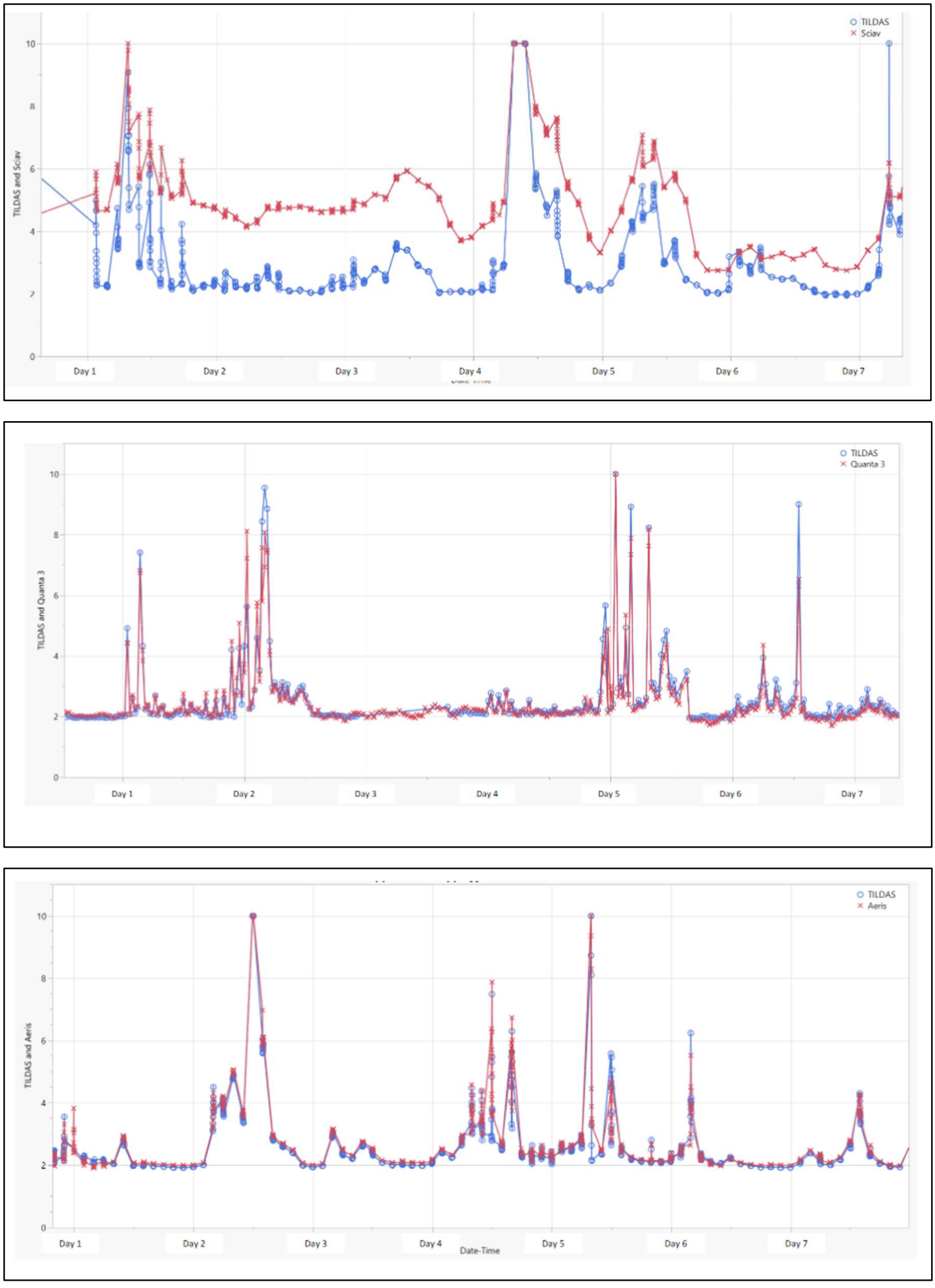

Figure 5-1. Comparisons of atmospheric methane concentrations measured by the QC-TILDAS system with the Scientific Aviation (upper), Quanta3 (middle) and Aeris sensors (Torres, et al., 2022)

While Figure 5-1 suggests a relatively stable background offset for the Scientific Aviation sensing system, field deployment indicated the possibility of rapid background changes. Figure 5-2 shows a comparison between co-located Scientific Aviation and Quanta3 sensing systems, with rapid background fluctuations for the Scientific Aviation sensing system that are not observed for the Quanta 3 sensing system.

Figure. 5-2-Month-long methane concentration time series for a metal oxide sensor with background fluctuations (upper), compared to a co-located infrared sensor with a more stable background (lower)

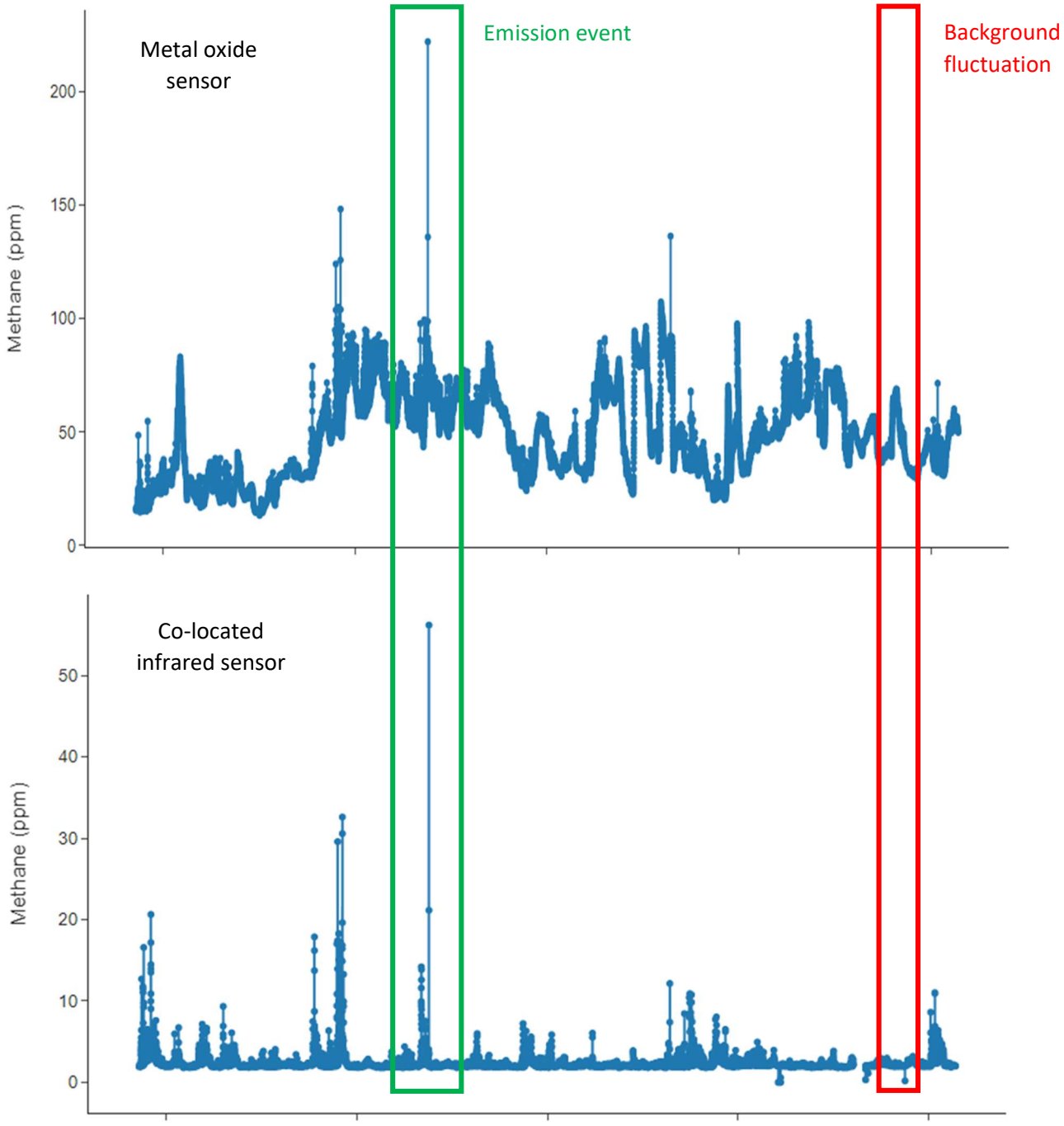

Multiple baseline correction algorithms were evaluated for the Scientific Aviation sensing system. Among the approaches that have been evaluated are:

Method 1: This background correction, recommended by the sensing system manufacturer, operates under the presumption that the location of an emission plume will vary significantly enough over a 15 minute period, so that the minimum concentration over a 15 minute period will be an effective background concentration for that 15 minute period. To calculate background adjusted methane concentration, the background concentration is subtracted from the raw concentration value of sensor. Then the assumed global background methane concentration (2 ppm) is added to the result. As shown in Figure 5-3, this approach can result in numerous false positive event detections if wind direction and relative humidity change significantly over a period of less than 15 minutes.

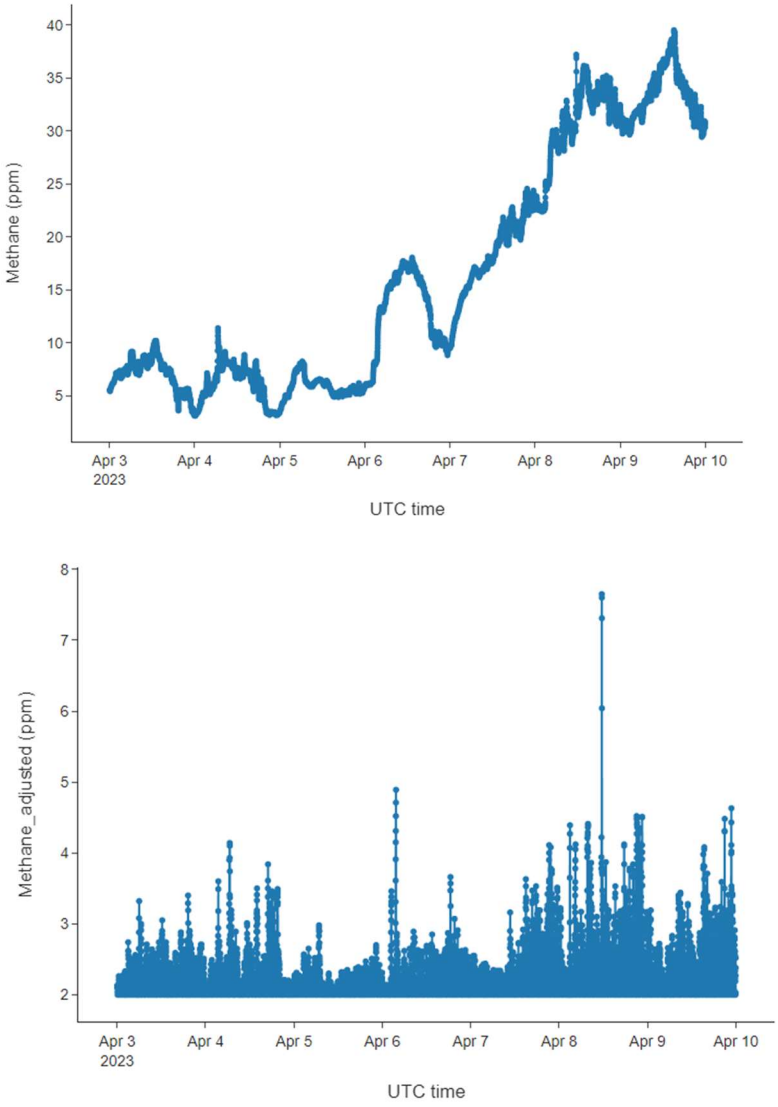

Figure 5-3. Absolute methane concentrations from the Scientific Aviation Soofie sensor (upper) and background corrected (Method 1) methane concentration (lower). Method 1 corrections, recommended by the vendor, is the minimum concentration over each 15 minutes period; this time period had relatively few events detected by collocated infrared sensors

Mehod 2: In this background correction, the predicting sensor background concentrations is estimated based on atmospheric temperature and humidity using a machine learning model developed at the University of Texas. The success of this approach depended on the learning data set. The approach was reasonably successful (see Figure 5-4) if the learning data set spanned the same time domain as the test data set, but if a learning data set was used to predict future data, the approach was far less successful, suggesting that background concentrations were being influenced by parameters other than temperature and relative humidity.

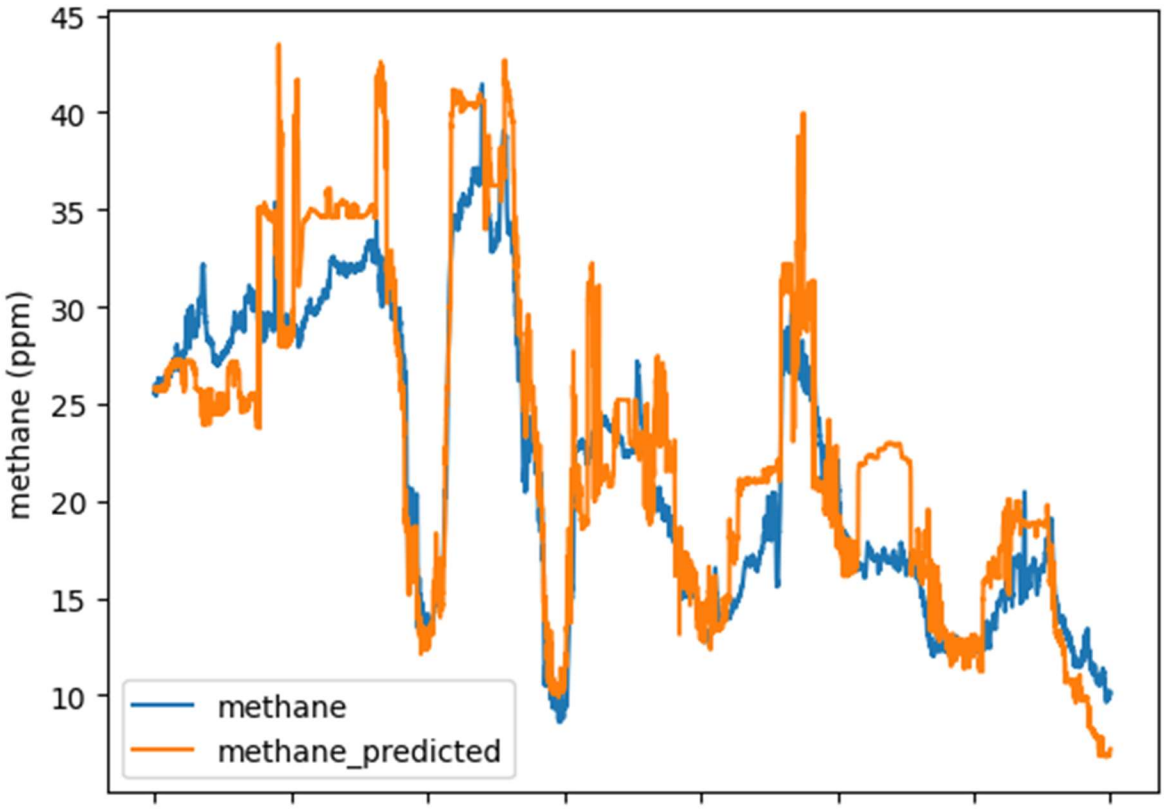

Figure 5-4. Background methane concentrations predicted by a machine learning model (Method 2).

Method 3: In this approach the background corrections estimated using Method 1 were compared across multiple sensors and were found to be highly correlated. Therefore, an initial background was calculated using Method 1 and was also calculated based on an estimate from a nearby sensor's absolute concentration, based on the correlation between sensors. An example of this background correction is shown in Figures 5-5, 5-6 and 5-7. While this resolved some of the issues with Method 1, it was observed that the correlations between sensors could evolve over time. This approach might also produce false negatives for very large emission plumes that are simultaneously observed by multiple sensors.

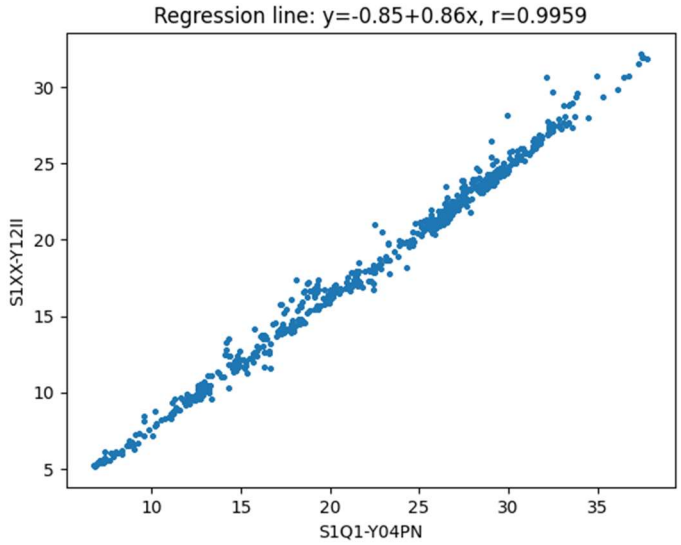

Figure 5-5. Representative correlation between background methane concentration, predicted using Method 1, for two Soofie sensors located on nearby sites. Background concentrations for many sensors had high degrees of correlations, but the correlations could vary over time and varied depending on when the sensor was acquired.

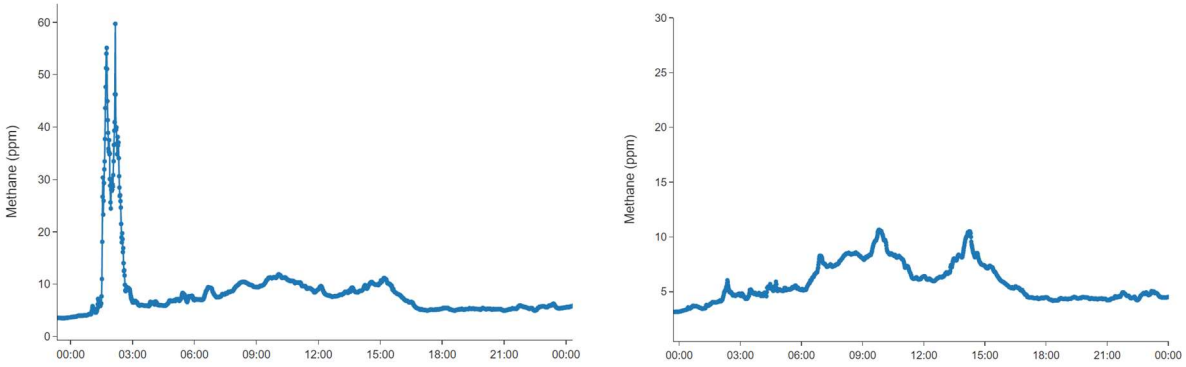

Figure 5-6. Methane concentrations without background correction for a sensor detecting an event (left) and concentrations for a nearby sensor with a highly correlated background concentration (right)

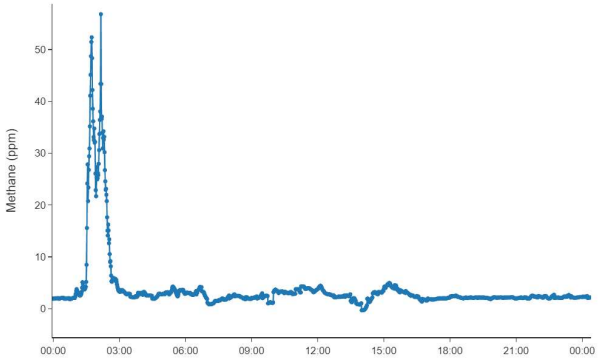

Figure 5-7. Background corrected sensor signal for the sensor in the left hand panel of Figure 5-6, based on the background detected by a nearby sensor (right hand panel in Figure 5-6)

Method 4: This approach combines emission event detection with background correction and compares rates of change in relative humidity to rates of change of methane concentration. This approach is still being evaluated, but shows promise.

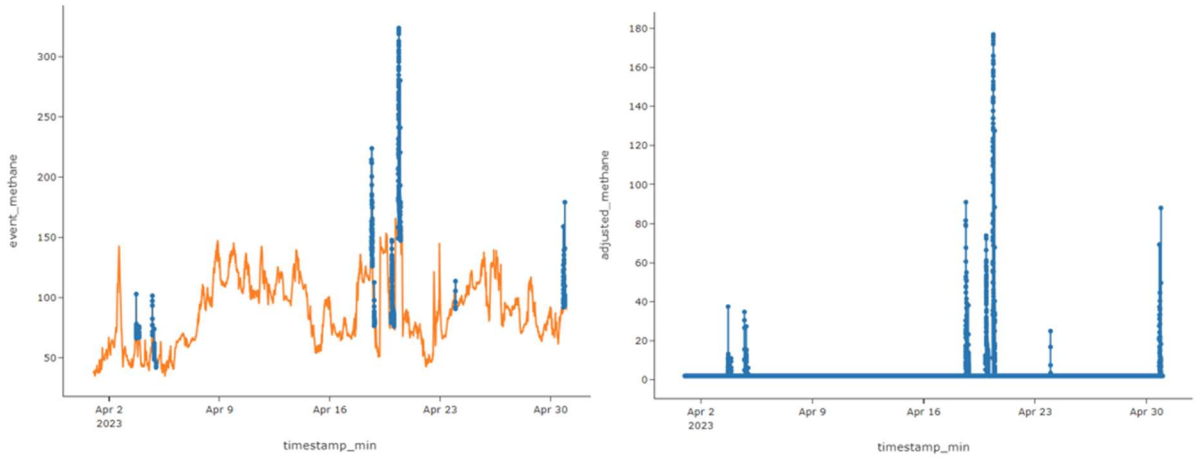

Figure 5-8. Events (blue lines) identified as periods when changes in methane concentration are not accompanied by a change in atmospheric water content.

Once signals are background corrected, a variety of algorithms for event detection can be applied to sensor data. Because of the on-going evaluation of background corrections, initial evaluations of event detection algorithms have utilized synthetic data, generated using atmospheric dispersion modeling. A typical scenario is illustrated in Figure 5-9. A centralized source on a pad has continuous emissions, generating a time series of methane enhancements at a sensor location, estimated using dispersion modeling.

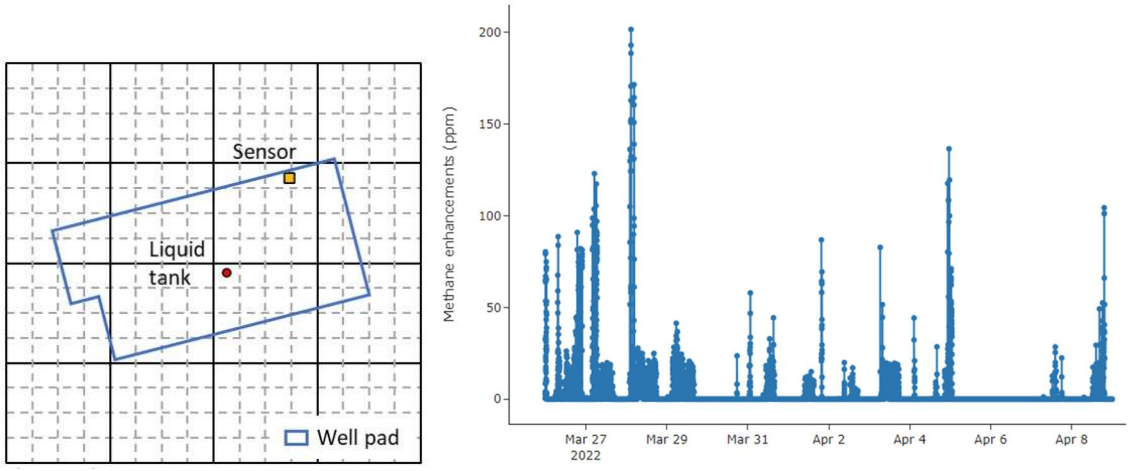

Figure 5-9. A liquid tank, located in the center of a pad (left) is assumed to emit at a rate of 100 kg/h, resulting in a signal at a sensor located on the pad (right); concentration enhancements due to the emission source, observed by the sensor, are estimated using dispersion model. The signal is used to evaluate event detection algorithms.

Three types of event detection have been evaluated:

1. Events defined based on the concentration enhancement exceeding a threshold
2. Rate of change of methane concentration exceeding a threshold
3. A time averaged concentration enhancement exceeding a threshold

Figure 5-10 shows results from methods 1 and 3, using the synthetic data illustrated in Figure 5-9. This work is beginning and will be expanded to include other algorithms and synthetic emissions.

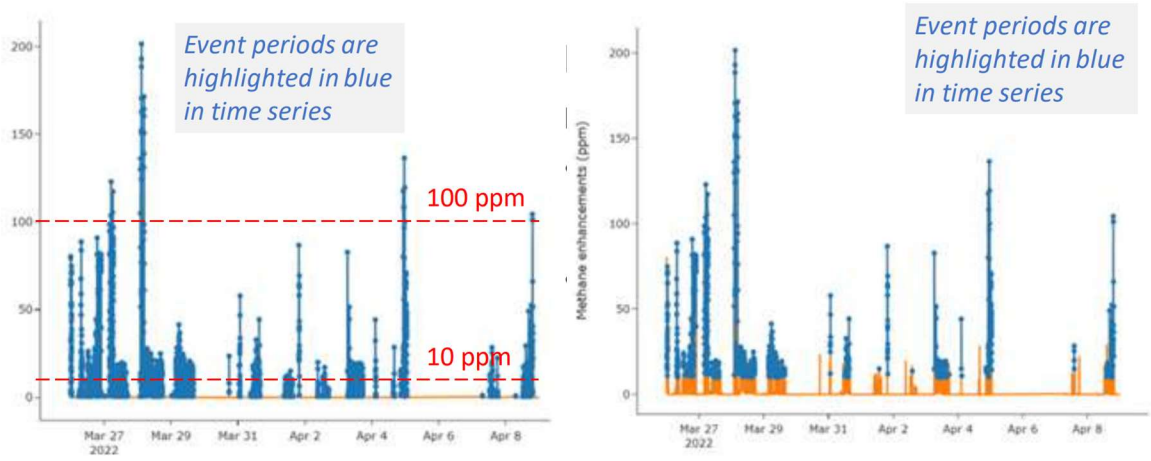

Figure 5-10. Two different methods for event detection applied to the same synthetic time series; the left panel shows a 10 ppm and 100 ppm concentration enhancement threshold applied to the synthetic time series of Figure 5-9. The right panel shows a time averaged threshold (an average of a 5 ppm enhancement over a 15 minute time period) for the same time series; the event detections are similar for the two methods.

5.2 Establishing event detection limits

The U.S. Environmental Protection Agency has established a minimum detection limit (MDL) for continuous monitoring systems (CMS) for methane emissions in its recent OOOOb/c regulations (U.S. EPA, 2023). That MDL is specified as 0.4 kg/s, however, because continuous monitoring systems do not directly measure emission rate, the detection limit of a CMS device is more accurately specified as a concentration enhancement detectable by a sensing system. Converting between MDLs based on emission rate remote from a sensor and concentration enhancement requires assumptions regarding meteorological conditions, the characteristics of emissions at the site, the positioning of CMS devices in relation to the emission sources, and the amount of time allowed for the CMS device to detect an emission source. A MDL based on emission rate is application and time period specific. Dispersion modeling was used to develop robust detection limit definitions for CMS (Chen, et al., 2024).

Dispersion modeling was performed based on deployment of sensors in a radial pattern, as shown in Figure 5-11. CMS devices locations were in concentric rings, with a sensor deployed every 45 degrees, at 10m, 20m, 30m, 40m and 50m from a source. The source was assumed to emit at the EPA defined emission threshold of 0.4 kg/hr, with a release height of 2.4 m agl. Sensors were assumed to be located at 2.4 m agl. Simulations were also performed at emission release heights of 5.5 m, which is representative of a release from the top of a storage tank.

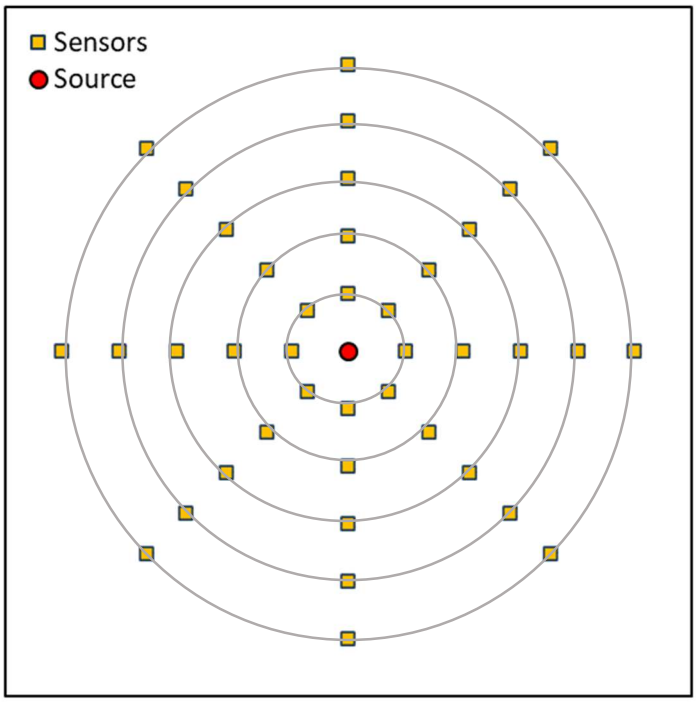

Figure 5-11. Source and sensor locations are deployed radially, in concentric rings every 45 degrees, at 10m, 20m, 30m, 40m and 50m from a source emiting at 0.4 kg/hr.

Dispersion modeling was performed using the same methods used to establish time to detection, described in Section 4. The procedures are described in detail by Chen, et al. (2024). The dispersion modeling simulations were used to generate mappings of the temporal coverage for various sensor configurations. Figure 5-12 shows the fraction of time that a 0.4 kg/hr emission

source with a release point located 2.4 m agl would be observed by at least one of 8 sensors deployed every 45 degrees, at 20 m from the source, if the detection threshold was set at 1000 ppb.

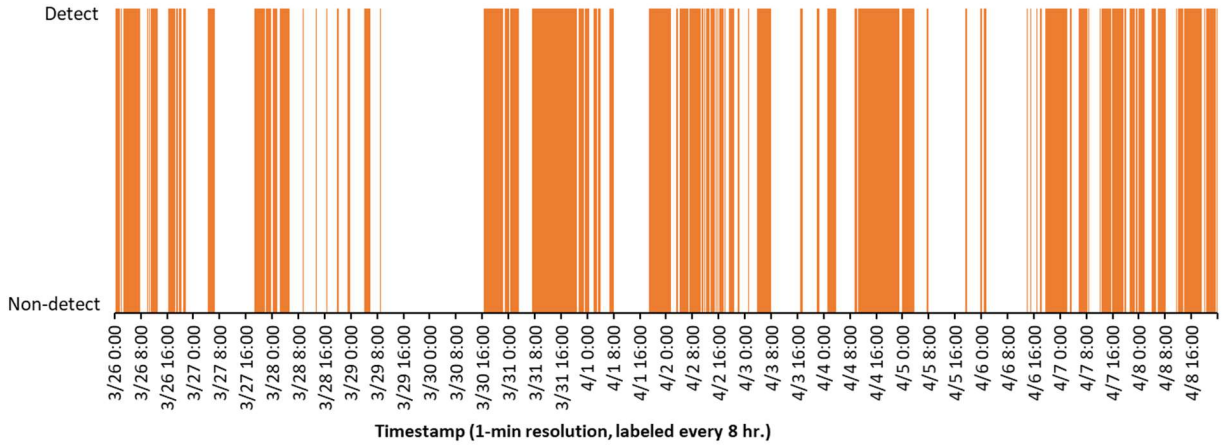

Figure 5-12. Time series of periods of detection and non-detection for a group of 8 sensors located 20 m from a source with a release rate of 0.4 kg/s and a release height of 2.4 m agl.

Similar time series were developed for multiple distances and detection thresholds. As shown in Figure 5-13, the temporal coverage depends on the concentration enhancement detectable by the sensing system and the distance from the source. At a 10 meter distance from the source, a sensing system able to detect a methane concentration enhancement of 2 ppm would detect emissions only about a quarter of the time, while a system capable of detecting a 200 ppb enhancement would detect emissions nearly all of the time.

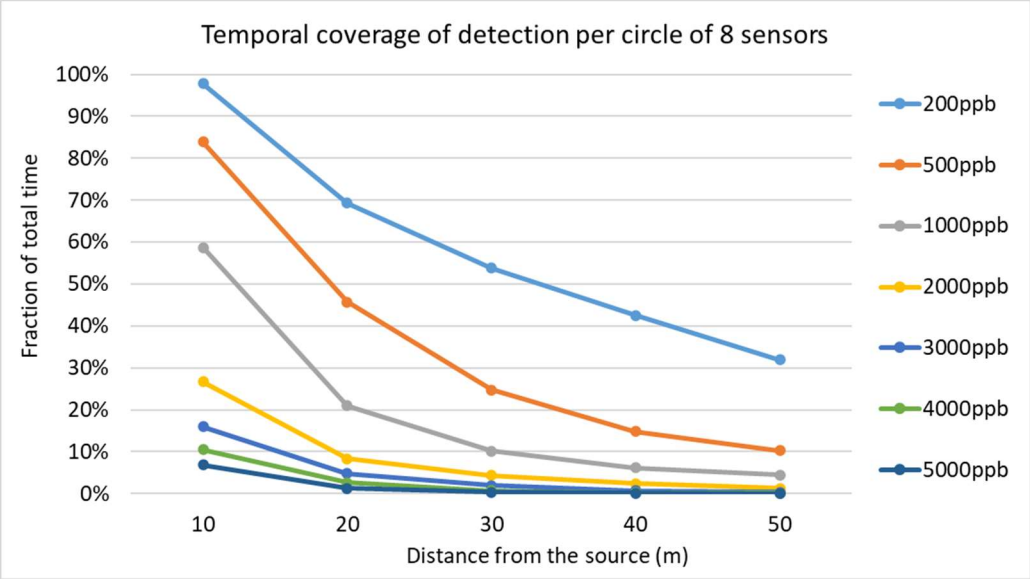

Figure 5-13. Fraction of time that a 0.4 kg/hr emission source with a release point located 2.4 m agl would be observed by at least one of 8 sensors deployed every 45 degrees at various distances from the source

If effectiveness is defined as a temporal coverage >30%, then only sensing systems with a detection threshold of 1 ppm or lower, at a 10-meter distance from the source, would be effective. If, however, effectiveness is defined using a time to detection metric, and effectiveness is defined as an average time to detection of 12 hours or less, then, as shown in Figure 5-14, systems with a wide range of detection thresholds up to 5ppm could be effective, at a 20-meter distance from the source. As shown in Figure 5, with lower detection limits (concentration enhancement threshold <2ppm), time to detection is more sensitive to detection thresholds rather than distance from the source.

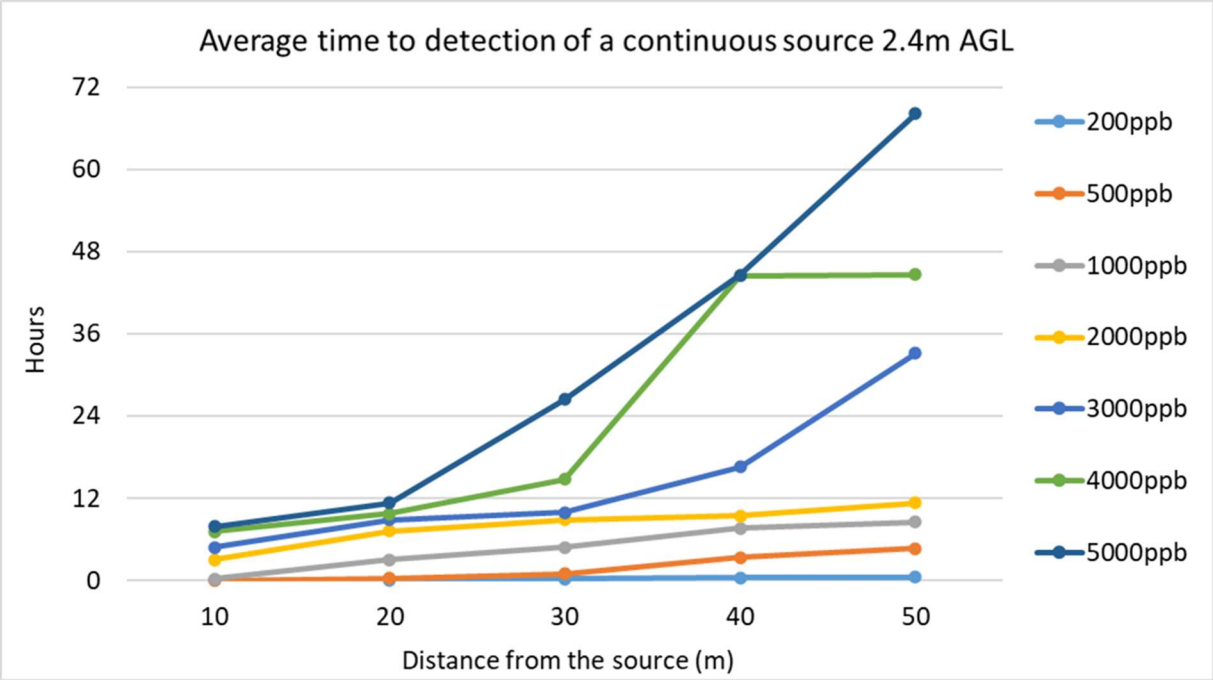

Figure 5-14. Detection times for a 0.4 kg/hr emission source with a release point located 2.4 m agl by a group of 8 sensors deployed every 45 degrees at various distances from the source

The dispersion modeling simulations performed using a source height of 2.4 m agl were repeated for a source height of 5.5 m agl. Results are described by Chen, et al. (2024). In general, temporal coverage was lower and time to detection higher, compared to the results for a source release height of 2.4 m. In addition, the relative performance of sensors between 10 and 20 m from the source was complex. For emission sources at the same height as the sensors (2.4 m agl), the temporal coverage and time to detection show relatively simple monotonic behavior, as illustrated in Figures 5-13 and 5-14. In contrast, for sources at 5.5 m agl, plumes may or may reach the sensor height at distances 10 m downwind, leading to complex detection characteristics depending on the methane concentration enhancement assumed for an emission detection and the meteorological conditions. This sensitivity to emission release height characteristics means that CMS performance and MDL will be sensitive to the mix of source characteristics.

The dispersion modeling demonstrates that the detection limit for continuous monitoring systems, expressed as an emission rate, will depend on meteorological conditions, the characteristics of

emissions at the site, the positioning of CMS devices in relation to the emission sources, and the amount of time allowed for the CMS device to detect an emission source. Work is on-going in developing systematic procedures for defining reproducible detection limit testing protocols.

5.3 Source attribution

Once an event is detected, the event is attributed to a source based on wind direction. There are multiple challenges associated with using wind directions to attribute emission events to sources. First, as shown in Figure 5-15, there may be multiple potential sources along a single back trajectory indicating the direction of flow from source to sensor. Figure 5-15 illustrates a scenario where winds are from the west southwest, with a back trajectory pointing from the east northeast. In this scenario, an event detected by sensor S4 could be from either of two sources along the back trajectory. Uncertainty in the distance from source to receptor will lead to uncertainties in emission quantification. It is possible to use additional characteristics of sensor signals at the site to distinguish between different sources along the same back trajectory. For example, the two sources that are on the same back trajectory when observed by sensor S4, would not be on the same back trajectory when observed by sensors S1 and S2. If the emission event persists until it can be detected by multiple sensors, a triangulation of the source position can be performed reducing uncertainty in source attribution. Nevertheless, using a wind direction from a single sensor at a single point in time will introduce uncertainty in source attribution.

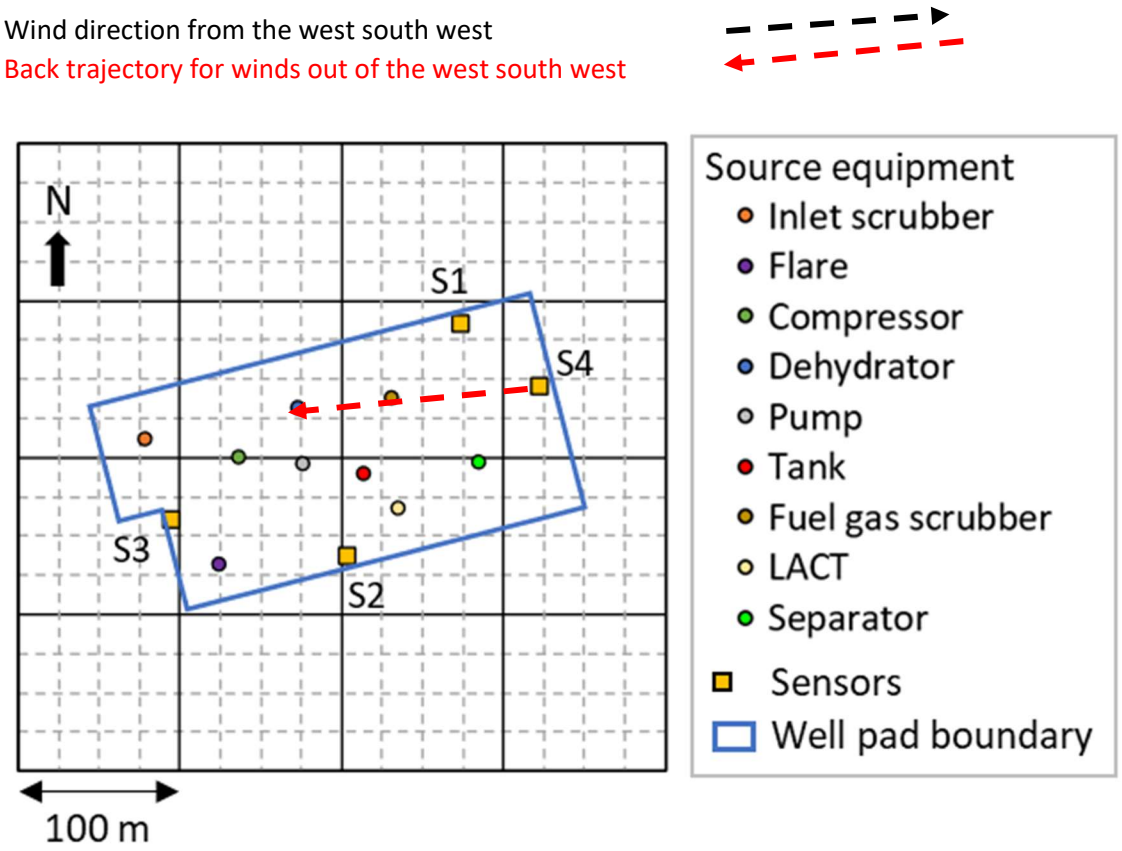

Figure 5-15. Multiple sources might occur along a single back trajectory, as shown for the back trajectory from sensor S4.

A second source of uncertainty in source attribution is variability in wind direction. Since wind direction can vary, even over the relatively short amount of time required for emissions plume to be transported from the source of emissions to the sensor, there is variability in the direction of transport from source to sensor. A single wind direction at a single moment in time may not indicate the true direction of transport. If an average distance from emission source to sensor is 40-200 meters and the average wind speed in the Permian Basin is 4 m/s (9 mph) then the average time for transport from source to receptor is 10-50 seconds. This uncertainty can be characterized by calculating the standard deviation of the wind direction, measured at 1 second intervals over a one-minute period. Data for the standard deviation of wind direction in the Permian Basin, measured at one second intervals over a one-minute period, as a function of wind speed, is shown in Figure 5-16. Variability in wind direction increases as wind speed decreases. Neglecting wind speeds below 2 m/s, most sub-minute scale variability in wind directions have a standard deviation of 10-15 degrees. This means that to capture 95% of typical variability in wind direction over a one minute period, a back trajectory cone would have a width of approximately 45 degrees.. This is shown conceptually in Figure 5-17.

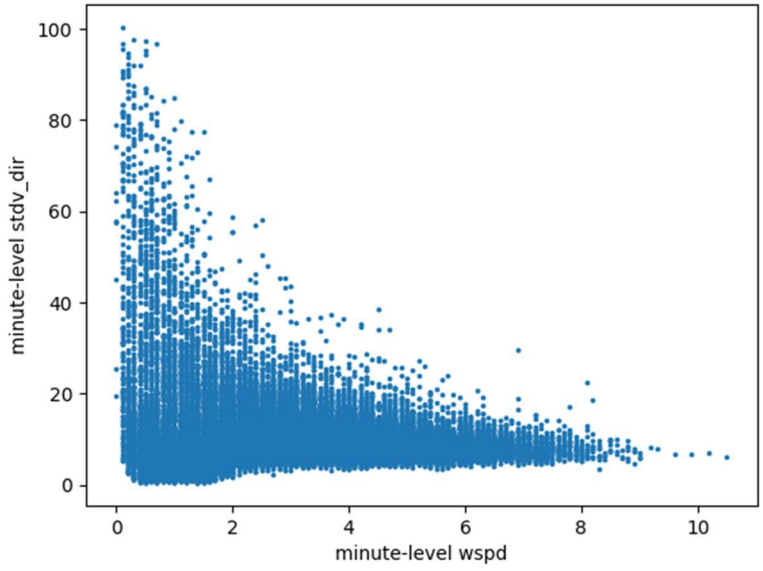

Figure 5-16. Standard deviation of one second resolution measurements of wind directions over a one minute averaging time, as a function of wind directions; measurements made at sensor locations in the Project Astra network

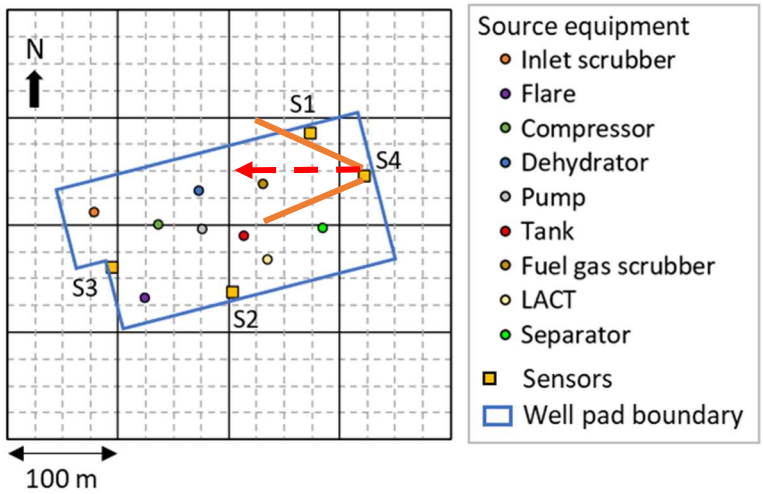

Figure 5-17. Band of possible emission source directions (red lines) associated with an easterly back trajectory (red arrow); the approximate 95% confidence limits of possible source directions span an angle of 45° due to short term (1 second) fluctuations in wind directions)

A third source of uncertainty in source attribution is due to plume width. As an emission plume is transported from source to sensor, the plume broadens, and the sensor may not detect the centerline of the plume. This means that taking the wind direction at the time of a detection event may generate a back trajectory that points toward the wrong source. This is shown conceptually in Figure 5-18. This source of uncertainty in source attribution will be greatest at low wind speeds when wind direction is also most variable. At higher wind speeds, sub-minute level variability in wind direction will allow sensors to sample multiple points in a plume, and by using wind directions at time of maximum observed concentration to calculate back trajectories, this uncertainty can be minimized.

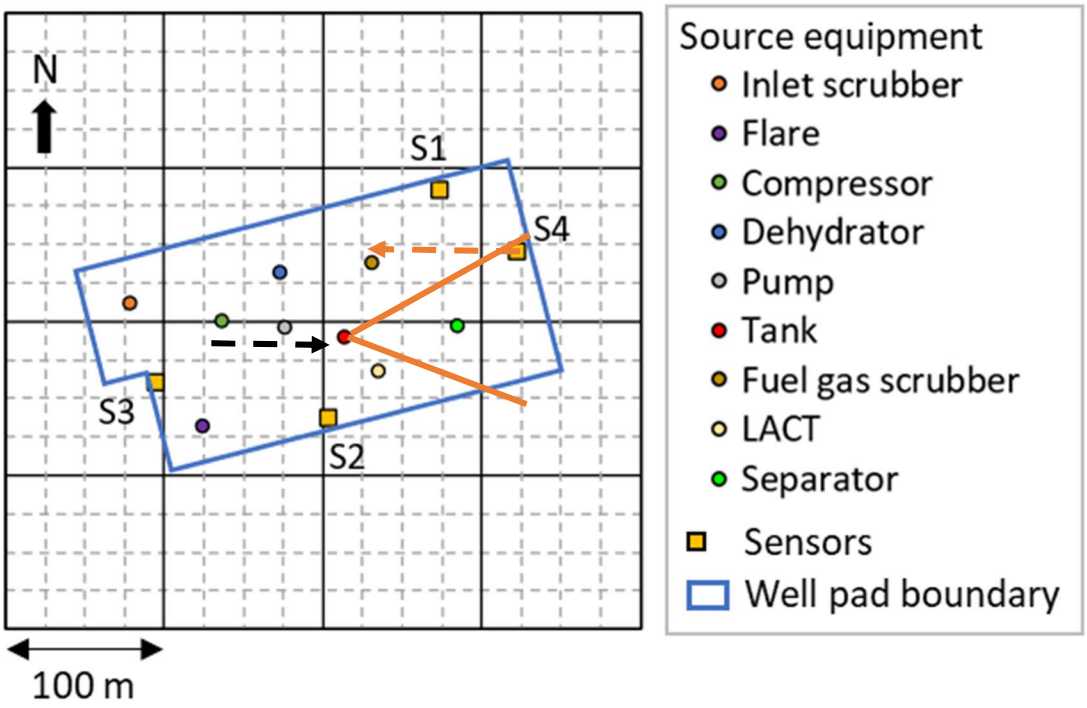

Figure 5-18. The outer edge of a plume released from the tank at the center of the site, with a wind from the west, is detected by sensor S4; if the back trajectory (red dashed line) is based on the wind direction, the source would be misidentified.

5.4 Emission rate quantification

Moving from a focus on emission event detection to emission quantification is an ongoing activity and will require improving the accuracy of (i) source attribution; (ii) event duration, and (iii) dispersion modeling.

Uncertainties associated with source attribution were described in Section 5.3. If the location of the source is not known accurately, then the distance to the source and the portion of the plume that a sensor is detecting will not be known. These uncertainties will both introduce uncertainties into the calculations used to convert a sensor signal into an estimated emission rate.

Uncertainties in event duration will be directly related to quantification of the mass released in an emission event. If there are large gaps in the signal from a source (see Figure 5-12), there will be uncertainties in estimating when an emission event began and when it ended, even if the emission rate can be precisely measured when the sensors are able to detect the source.

Once an event is detected, dispersion models are used to convert the concentration enhancement detected by the sensor into an emission rate. This requires accurate dispersion modeling. To perform a preliminary assessment of the accuracy of relationship between emission rates and sensor observed concentrations, four different formulations of dispersion models, each using the same input data, were used to simulate the emission scenario illustrated in Figure 5-9. The results are illustrated in Figure 5-19. This simple example illustrates that a single emission rate might be associated with concentrations at a sensor that could vary by a factor of 2-5 or more, depending on conditions.

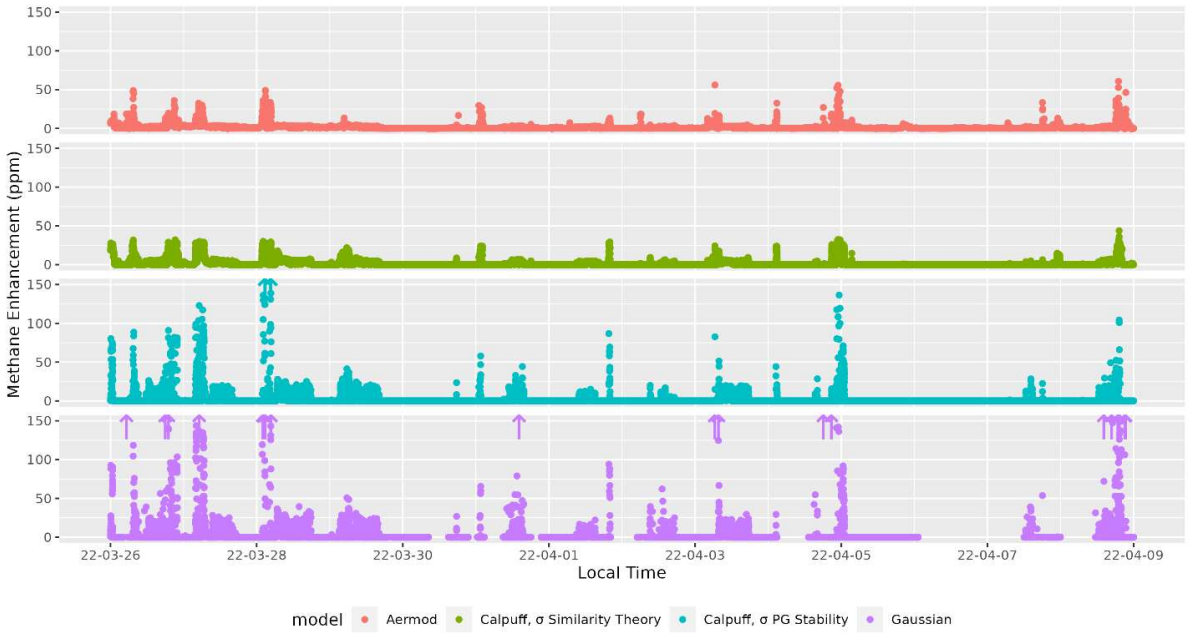

Figure 5-19. Predictions of observed sensor concentrations for the case study illustrated in Figure 5-9, using four different dispersion model formulations [PG = Pasquill-Gifford method of calculating dispersion coefficients]; the concentration to emission rate ratio can vary by a factor of 2-5 or more, depending on conditions. Upward arrows indicate predictions beyond the vertical scale.

6. Overall performance

The overall Project Astra technology readiness assessment (TRA) system is illustrated in Figure 6-1, where critical components are highlighted in yellow.

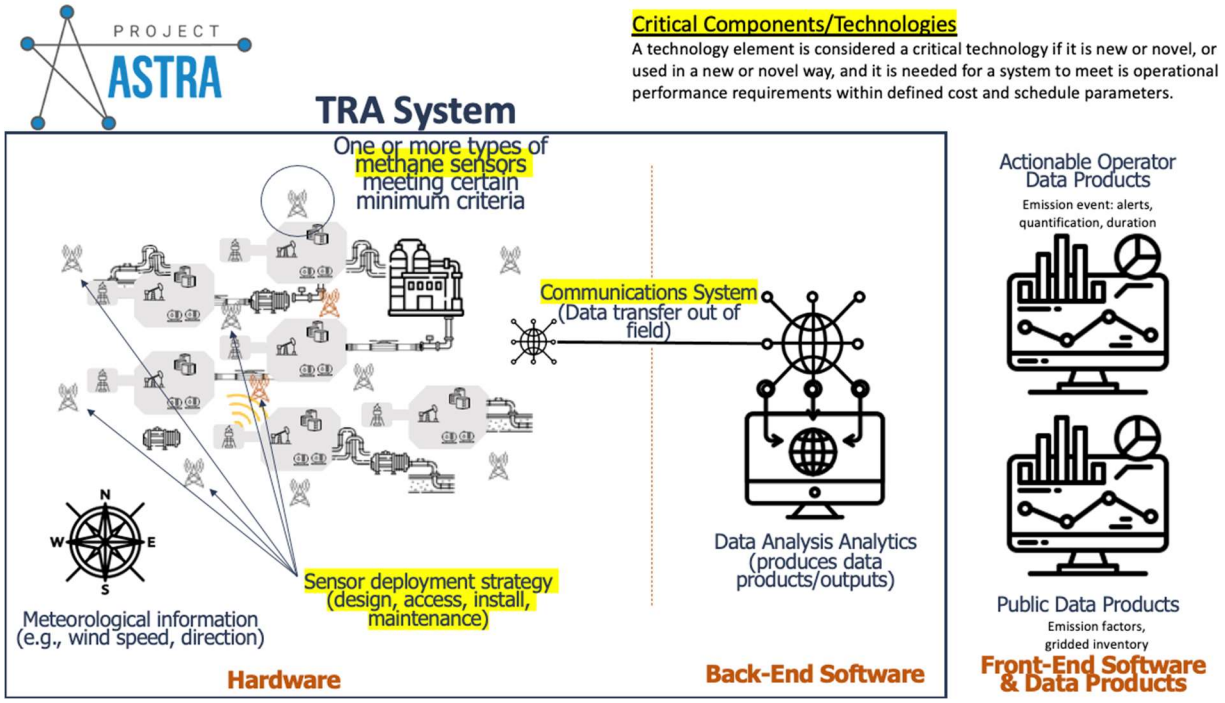

Figure 6-1. Project Astra technology readiness assessment (TRA) system with critical components highlighted in yellow

The overall status of the system components is summarized in Table 6-1. As described in Table 6-1, commercial methane sensing systems have different characteristics and different cost and performance levels, but multiple systems are commercially available. Sensor deployment strategies are also at a relatively mature level, as described in Section 4. Communications systems, as part of the sensing systems are already integrated into commercial products, although communications coverage may still be challenging in some remote areas. Meteorological data collection systems are commercially available, however, while the data are broadly available, the data analytics systems needed to use these data in emission detection and quantification still requires improvement as described in Section 5. Improving data analytics is the main focus of the ongoing work of Project Astra.

Table 6-1. Technology readiness summary (TRA) for Project Astra subsystems

Individual Subsystem	Critical component	Current TRL	Target TRL	Comments
Methane Sensors	Yes	9	9	Commercially functional under relevant conditions as independent systems.
Sensor Deployment Strategy	Yes	6	7	Demonstrated in pilot scale for a partial deployment (upstream only).
Meteorological information collection	No	9	9	Commercially functional under all relevant conditions.
Communication systems	Yes	7	7	Commercially functional, but no single communication system is continuously available throughout entire commercial target domain.
Project Astra TRA		6	7	Sensor network has been deployed in a relevant environment at a prototypical pilot scale for some time, the operating system is still relatively "low fidelity" compared to the eventual system

References

Chen, Q., Modi, M., McGaughey, G.M., Kimura, Y. McDonald-Buller, E.C., Allen, D.T., Simulated methane emission detection capabilities of continuous monitoring networks in oil and gas production regions, *Atmosphere*, 13(4), 510, doi: 10.3390/atmos13040510 (2022).

Chen, Q., Schissel, C., Kimura, Y., McGaughey, G., McDonald-Buller, E.C. Allen, D.T., Assessing detection efficiencies for continuous methane emission monitoring systems at oil and gas production sites, *Environmental Science & Technology,* 57, 1788–1796 doi: 10.1021/acs.est.2c06990 (2023a).

Chen, Q., Kinura, Y., and Allen, D.T., Determining times to detection for large methane release events using continuously operating methane sensing systems at simulated oil and gas production sites, submitted to *Environmental Science & Technology Letters*, preprint at ChemRxiv, doi: 10.26434/chemrxiv-2023-p8lfk (2023b).

Chen, Q., Kinura, Y., and Allen, D.T., Defining detection limits for Continuous Monitoring Systems for methane emissions at oil and gas facilities, in preparation (2024).

Texas Commission on Environmental Quality (TCEQ), 2024. CAMS 47 monitoring site; U.S. Environmental Protection Agency Air Quality System (AQS) ID 481350003; data available at: https://www17.tceq.texas.gov/tamis/index.cfm?fuseaction=report.view_site&siteID=180&siteOrderBy=name&showActiveOnly=0&showActMonOnly=1&formSub=1&tab=info accessed January 26, 2024.

Torres, V.M., Sullivan, D.W., He'Bert, E., Spinhirne, J., Modi, M., Allen, D.T., Field inter-comparison of low-cost sensors for monitoring methane emissions from oil and gas production operations, Preprint amt-2022-24 (2022).

United States Environmental Protection Agency, (US EPA 2023b) Standards of Performance for New, Reconstructed, and Modified Sources and Emissions Guidelines for Existing Sources: Oil and Natural Gas Sector Climate Review, available at: https://www.epa.gov/system/files/documents/2023-12/eo12866_oil-and-gas-nsps-eg-climate-review-2060-av16-final-rule-20231130.pdf accessed December 26, 2023.